Since January 2020 Elsevier has created a COVID-19 resource centre with free information in English and Mandarin on the novel coronavirus COVID-19. The COVID-19 resource centre is hosted on Elsevier Connect, the company's public news and information website.

Biochemical and Biophysical Research Communications 606 (2022) 17–22

Contents lists available at ScienceDirect

Biochemical and Biophysical Research Communications

journal homepage: www.elsevier.com/locate/ybbrc

Structural insights revealed by crystal structure of B38-CAP, an isoenzyme of carboxypeptidase ACE2, the receptor of SARS-CoV-2

Peiyuan Liu [a, 1], Yanfeng Zhang [a, 1], Zibin Li [c], Jianwen Huang [b, ***], Tao Wang [a, **], Cheng Chen [a, *]

[a] School of Life Sciences, Tianjin University, Tianjin, 300072, PR China
[b] State Key Laboratory of Biocatalysis and Enzyme Engineering, School of Life Sciences, Hubei University, Wuhan, 430062, PR China
[c] Tianjin Key Laboratory of Agricultural Animal Breeding and Healthy Husbandry, College of Animal Science and Veterinary Medicine, Tianjin Agricultural University, Tianjin, 300384, PR China

ARTICLE INFO

Article history:
Received 6 March 2022
Accepted 15 March 2022
Available online 18 March 2022

Keywords:
SARS-CoV-2
Renin-angiotensin system
ACE2 carboxypeptidase
B38-CAP
Isoenzyme

ABSTRACT

The worldwide pandemic of Coronavirus disease 2019 (COVID-19) is triggered by severe acute respiratory syndrome coronavirus 2 (SARS-CoV-2) and further worsened by the emergence of a variety of SARS-CoV-2 variants. Angiotensin-converting enzyme 2 (ACE2), a carboxypeptidase of M32 family, serves as the receptor of SARS-CoV-2 and key regulator of host renin-angiotensin system (RAS), both of which are mainly mediated via the carboxypeptidase domain of ACE2 (sACE2) or its activity. sACE2 is thus promising in the treatment of COVID-19 but unfortunately weakened by its unstrigent substrate preference and complex interplay with host RAS. B38-CAP, an isoenzyme of ACE2, partically compensates these defects but still encounters the problem related to carboxypeptidase activity and specificity. In this study, we firstly determined the crystal structure of B38-CAP at a resolution of 2.44 Å which exists in dimeric form with the non-crystallographic two-fold axis being in coincidence with the crystallographic two-fold axis. Further structural analysis revealed the structural conservatism feature among M32 family, particularly the catalytic core and moreover lead us to hypothesize that conformational flexibility might play an pivotal role in the catalysis of B38-CAP and ACE2. The work provided here presents key features of the M32 family carboxypeptidase and provides structural basis for further development of B38-CAP-based anti-SARS-CoV-2 drugs.

1. Introduction

The worldwide pandemic of Coronavirus disease 2019 (COVID-19), which is triggered by severe acute respiratory syndrome coronavirus 2 (SARS-CoV-2) [1], a member of genus *betacoronavirus* within the subfamily *Orthocoronavirinae* [2], has caused about 435 million infections and more than 59 hundred thousand deaths as of March 3, 2022 [3]. To combat SARS-CoV-2 infection, a series of vaccines, neutralizing antibodies as well as small-molecule drugs have been developed and/or approved [4–8]. However, with the ongoing and repeated spreading of SARS-CoV-2 in the global world, a number of genetic variants of SARS-CoV-2 have emerged, due to its intrinsic property of being prone to genetic mutation while infecting and adapting to human hosts [9]. These variants display considerably different characteristics compared to their ancestral strains, which have been leading to the compromised efficacy of approved vaccines and probably those antibodies and small molecule drugs, hence strengthening the ever-growing demand of developing broad-spectrum drugs against SARS-CoV-2 mutants [10].

Angiotensin-converting enzyme 2 (ACE2), a single transmembrane protein characterized of a carboxypeptidase domain belonging to M32 carboxypeptidase family [11], has been thought to meet the aforementioned need of wide-spectrum anti-SARS-CoV-2 drug development due to its multiple functions in SARS-CoV-2 pathogenesis [12,13]. During the course of SARS-CoV-2 infection, ACE2 (or more specifically, its membrane-bound form) firstly serves as the receptor of SARS-CoV-2. To enter into host cells,

* Corresponding author. School of Life Sciences, Tianjin University, No.92 Weijin Road, Nankai District, Tianjin, 300072, PR China.
** Corresponding author.
*** Corresponding author.
E-mail addresses: huangjianwen@hubu.edu.cn (J. Huang), wangtaobio@tju.edu.cn (T. Wang), chengchen@tju.edu.cn (C. Chen).
[1] Theses authors contributed equally to this work.

https://doi.org/10.1016/j.bbrc.2022.03.077
0006-291X/

the receptor binding domain (RBD) of SARS-CoV-2 Spike protein needs to first bind to the carboxypeptidase domain of ACE2, immediately followed by the cleavage of Spike protein by TMPRSS2 [12,14]. In the meantime, ACE2, as a key regulator of host renin-angiotensin system (RAS), also employs its carboxypeptidase activity to reduce host inflammatory response and restrict the deterioration of SARS-CoV-2 [13,15]. This is also mediated by the carboxypeptidase domain of ACE2 through the digestion of substrate Ang II to Ang (1–7), despite a dozens of other substrates having been identified for ACE2 [16]. Thus, the soluble carboxypeptidase domain of ACE2 (sACE2) which possesses both RBD-binding (in other way, SARS-CoV-2 neutralizing) and RAS-modulating ability regardless of whether and how SARS-CoV-2 mutates, is a natural drug candidate to treat COVID-19. Currently, a series of sACE2-based anti-SARS-CoV-2 strategy are in investigation [17–19]. However, it's not until recently that researchers find that sACE2 surprisingly mediate the cell entry of SARS-CoV-2 via interaction with proteins related to RAS [20]. This finding, in addition to indicating the antagonistic role of ACE2 in SARS-CoV-2 pathogenesis, further promotes people to re-examine the clinical complexity of ACE2.

B38-CAP, another member of M32 carboxypeptidase family and in fact an isoenzyme of ACE2's carboxypeptidase domain, serves as a better start for developing anti-SARS-CoV-2 drug, due to its non interacting property with RAS proteins and moreover, an extra ability of digesting Ang(1–9) into Ang(1–8) compared to ACE2 [21]. However, B38-CAP is found to display weaker carboxypeptidase activity compared to ACE2 and retain the shortcoming of unstrigent substrate property of ACE2 [21]. To aids our understanding of the carboxypeptidase activity of B38-CAP, we firstly determined the three-dimensional structure of B38-CAP in this study and then performed structural comparison between B38-CAP and other M32-family carboxypeptidases, particularly ACE2. It was shown that B38-CAP which exists in dimeric form shares structural rather than sequence conservatism with ACE2 particularly in the catalytic core, while in the meantime, displays little structural flexibility in dimeric form compared to ACE2, which may have a potential effect and thus contribute to their difference in carboxypeptidase activity.

2. Materials and methods

2.1. Expression and purification

The coding sequence of B38-CAP was synthetized and cloned into the vector pGEX-6P-1 (GE Healthcare) using the *Bam*H I and *Xho*I restriction sites. After veried by sequencing, the recombinant plasmid was transformed into *Escherichia coli* strain BL21 (DE3) for protein expression. Cultures were grown in LB medium containing 0.1 mg/mL ampicillin at 310 K until the optical density at 600 nm reached 0.8. Isopropyl-ß-D-thiogalactopyranoside at a final concentration of 0.5 m*M* was then added to the cultures and a total time of 16 h was applied at 289 K to induce to expression of recombinant B38-CAP with an N terminal GST tag. Thereafter, centrifugation was used to harvest the cells and the bacterial pellets, after resuspended in TBS (25 mM Tris-HCl, pH 8.0, 150 mM NaCl), was disrupted using high-pressure homogenizers. The lysate of the bacteria was centrifuged at 18,000 rpm for 50 min at 277 K. The supernatant was then loaded onto a disposable column containing glutathione sepharose 4B affinity resin (GE Healthcare) for purifying GST-tagged B38-CAP protein. The fusion protein, after washed with 6 columns of TBS buffer, was then subjected to on-column cleavage using commercial PreScission protease at 277 K for 12 h. The protease was added to a final concentration of 0.25 mg/mL.The resulting protein of interest was eluted and purified by anion-exchange chromatography using a Source Q column (GE Healthcare) and further characterized by size-exclusion chromatography using a Superdex™ 200 Increase 10/300 GL column (GE Healthcare) in a buffer containing 10 mM Tris-HCl pH 8.0, 100 mM NaCl. The final protein reached more than 95% purity by SDS-PAGE analysis and qualified for crystallographic analysis.

ACE2 carboxypeptidase domain spanning residues 19–615 was expressed using the Bac-to-Bac baculovirus system (Invitrogen). Basically, the coding sequence of ACE2 carboxypeptidase domain with an N-terminal GP67 signal peptide and a C-terminal His tag was cloned into pFastBac-Dual vector (Invitrogen). The constructed plasmid, after sequenced for verification, was then transformed into bacterial DH10Bac competent cells for extracting corresponding bacmid which was then transfect into Sf9 cells using Cellfectin II Reagent (Invitrogen). The low-titre viruses were collected and then amplified to generate high-titre virus stocks, which were used to infect Hi5 cells at a density of 1.8×10^6 cells per mL. The supernatant of cell culture containing the secreted ACE2 was collected 72 h after infection. The ACE2 carboxypeptidase domain was captured by Ni resin (GE Healthcare) and eluted with 300 mM imidazole in lysis buffer (25 mM Tris-HCl, pH 8.0,150mM NaCl), then purified by size-exclusion chromatography method using a Superdex™ 200 Increase 10/300 GL column (GE Healthcare) in a buffer containing 10 mM Tris-HCl, pH 8.0, 100 mM NaCl.Fractions containing the ACE2 were collected [14].

2.2. Crystallization

The purified B38-CAP protein was concentrated to 20 mg/mL in the above buffer containing 10 mM Tris-HCl, pH 8.0, 100 mM NaCl. In the primary stage, commercial kits including were used to screen for preliminary crystallization conditions for B38-CAP. Crystallization trials were set in 48-well crystallization plates at 291 K using the sitting-drop vapour diffusion method. Crystallization drops were carefully set by mixing 1.0 μL protein solution with 1.0 μL of the reservoir solution and then left to equilibrate with 80 μL reservoir solution. Initial crystals of B38-CAP protein were obtained after 24 h under multiple conditions. The crystals used for diffraction data collection grew in the optimized solution containing 0.1 M Tris-HCl pH8.5, 1.0 M Sodium citrate.

2.3. Data collection and processing

B38-CAP crystals were cryoprotected in a solution containing 1.0 M Sodium citrate, 0.1 M Tris-HCl, pH 8.5 supplemented with 10% glycerol and then mounted in a nylon loop and flash-cooled in a nitrogen stream at 100 K. The X-ray diffraction data sets were collected using an R-AXIS IV++ image-plate system and an in-house rotating-anode Cu generator (Rigaku, USA) at a wavelength of 1.5418 Å. The crystals showed high-quality diffraction patterns. All intensity data were indexed, integrated and scaled with the *HKL-3000* package. A complete data set diffracting to 2.0 Å was collected and the related data collection and processing statistics are summarized in Table 1.

2.4. Structure solution, refinement and analysis

The crystal structure of B38-CAP was solved by molecular replacement method in *Phaser* using the structure of BsuCP (PDB entry 3HQ2) as the search model [22]. The initial model was then subjected to manual rebuilt in *COOT* [23] and automatic refinement in *PHENIX* [24] iteratively until the stereochemical parameters suit the criteria of *Molprobity* [25]. The refinement strategy includes individual_sites refinement in real-space and reciprocal-space, atomic displacement refinement and TLS refinement. In the final stage of refinement, solvent molecules were added at a contour

Table 1
Data collection and refinement statistics.

Parameters	B38-CAP
X-ray Source	Rigaku MicroMax-007 HF
Wavelength (Å)	1.5418
Space group	*C*2
Unit cell parameters (Å; °)	a = 106.6, b = 70.0, c = 88.2; α = γ = 90.0, β = 112.3
Resolution range (Å)	50.0–2.44 (2.49–2.44)[a]
Unique reflections	21,932 (873)
Completeness (%)	96.4 (77.4)
Redundancy	3.0 (2.7)
I/σ(I)	40.2 (11.1)
R_{merge} (%)	2.3 (10.0)
$CC_{1/2}$	0.999 (0.985)
Refinement statistics	
Resolution range (Å)	42.61–2.437 (2.524–2.437)
Reflections used in refinement	21,930 (2,065)
Reflections used for R-free	1,110 (105)
R_{work} (%)	16.9 (20.0)
R_{free} (%)	20.1 (24.9)
Number of non-hydrogen atoms	4,226
Protein	4,070
Solvent	154
Ligand	2
Average B-factors	38.5
Protein	38.5
Solvent	38.7
Ligand	42.7
r.m.s. deviations	
Bond lengths (Å)	0.007
Bond angles (°)	0.89
Ramachandran	
Favored (%)	97.8
Allowed (%)	2.2
Outliers (%)	0.0

[a] Values for the outer shell are given in parentheses.

level of 3.0 σ. Structural comparison were performed using the *DALI* program [26]. The figures were prepared in molecular graphics system *PyMOL* [27].

2.5. In vitro carboxypeptidase activity measurements

The real-time measurement of the carboxypeptidase activity of B38-CAP and ACE2 carboxypeptidase domain was investigated using Nma-His-Pro-Lys(Dnp) as the fluorescent substrate using the EnSpire Multilabel Plate Reader (PerkinElmer, USA). The reaction mixture contained 40 μL of 0.1 M HEPES pH 7.5, containing 0.3 M NaCl, 0.01% Triton X-100, 80 μM fluorescent substrate, and 0.0125 μg of B38-CAP protein or ACE2 carboxypeptidase domain in a total volume of 50 μL. The reaction mixture was incubated at 37 °C for 1 min and then measured spectrophotometrically at an emission wavelength 440 nm upon excitation wavelength 340 nm on an EnSpire multilabel plate reader [28].

3. Results and discussion

3.1. Characterization of the oligomeric state and carboxypeptidase activity of B38-CAP

B38-CAP and ACE2 carboxypeptidase domain were expressed using *E.coli* and Bac-to-Bac baculovirus system, respectively. To investigate their oligomeric state, gel-filtration characterization using a Superdex™ 200 Increase 10/300 GL column was performed and the elution volume for B38-CAP and ACE2 carboxypeptidase domain was calibrated as 14.2 and 13.2 mL, respectively, indicating that B38-CAP, unlike ACE2 carboxypeptidase domain, exists in dimeric instead of monomeric form in solution (Fig. 1A). Their carboxypeptidase activity was then measured by the fluorescent method. It's noteworthy that an real-time mode is employed here rather than the average mode reported in earlier literature [21]. It turns out that B38-CAP displays considerably weak carboxypeptidase activity compared to ACE2 carboxypeptidase domain (Fig. 1B), rasing the concern that how this can be linked to their respective structural differences.

3.2. The overall structure of B38-CAP

The crystal structure of B38-CAP which belongs to *C*2 space group was solved to a resolution of 2.44 Å by molecular replacement method using the program *Phaser* and finally refined an R_{work}/R_{free} factor of 15.6% and 20.0% respectively. The final structure consists of 30 α/η-helices and 3 β-sheets, with one molecule per asymmetric unit, seeming contradictory to gel-filtration profile of B38-CAP. A fine inspection of crystal packing reveals that the non-crystallographic two-fold axis between the two molecules of B38-CAP dimer is in perfect coincidence to the crystallographic two-fold axis of the *C*2 space group (Fig. 2A). The interface area between the two molecules constituting B38-CAP dimer is as high as 984.5 $Å^2$. An extensive hydrogen bond, salt bridge and hydrophobic interaction network exists between these two B38-CAP molecules, contributing to the stabilization of B38-CAP dimer (Fig. 2B). Inside of the structure, there is a zinc ion, which, by coordination with residues H269, H273, E273 and water molecules, forms the catalytic core (Fig. 2A). To assess the conservative property of B38-CAP, we then performed *DALI* structural similarity search and identified eight M32 carboxypeptidase in PDB database, all bacteria-derived, with r.m.s. deviation between them ranging from 1.1 to 2.9 Å (Table S1). Structural alignment clearly shows that B38-CAP adopts a typical M32 carboxypeptidase domain fold (Fig. 2C). This is in good accordance with the sequence comparison result, which means B38-CAP and the eight carboxypeptidases share both structural and sequence conservation (Table S1).

3.3. The structural conservation and diversity between B38-CAP and ACE2

Sequence comparison displays little, if there is, identity between B38-CAP and ACE2 carboxypeptidase domain (Fig. 3A), raising the question that whether ACE2 has evolved a brand-new model for carboxypeptidase catalysis. Considering that structural conservatity is more reliable, a *DALI* analysis was performed using the structure of B38-CAP monomer and ACE2 carboxypeptidase domain, which however gives an r.m.s. deviation of 5 Å with 437 Cα atoms aligned. It's surprising to find that further inspection of their fine structure reveals that the catalytic core of B38-CAP and ACE2 are completely conservative between each other and so is the spatial configuration of the structural elements adjacent to catalytic core (Fig. 3B). This strongly indicates that the catalytic core of M32-family carboxypeptidases was strictly reserved during their evolution process, which however poses a confusion for us to understand the differences displayed in their carboxypeptidase activity, until we surprising find that all and only bacteria-derived carboxypeptidase adopts dimeric form. As shown in Fig. 4, the dimeric property is strictly conservative among B38-CAP and the above eight bacteria-derived carboxypeptidases, albeit a little bit flexibility is revealed in distal end compared to the tight state in the dimeric interface. On contrast, ACE2 has evolved at least two states, namely open and closed state which are indispensable for efficient catalysis [29]. This marked difference promotes us to reasonably infer that liberation of ACE2 into monomeric state during its evolution process might contribute to its higher efficiency during

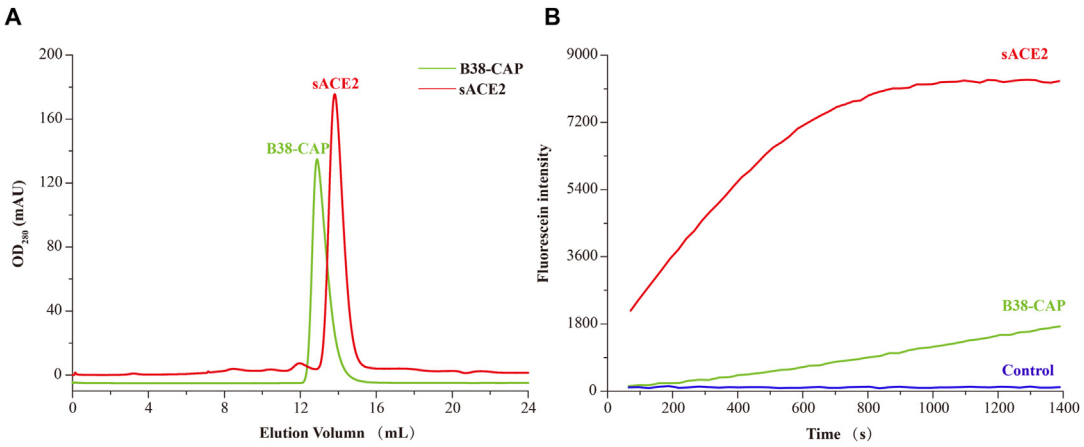

Fig. 1. Characterization of the oligomeric state and carboxypeptidase activity of B38-CAP and ACE2 carboxypeptidase domain. **(A)** The gel-filtration profile of B38-CAP and ACE2 carboxypeptidase domain in a Superdex™ 200 Increase 10/300 GL column. **(B)** Real-time characterization of the carboxypeptidase activity of B38-CAP and ACE2.

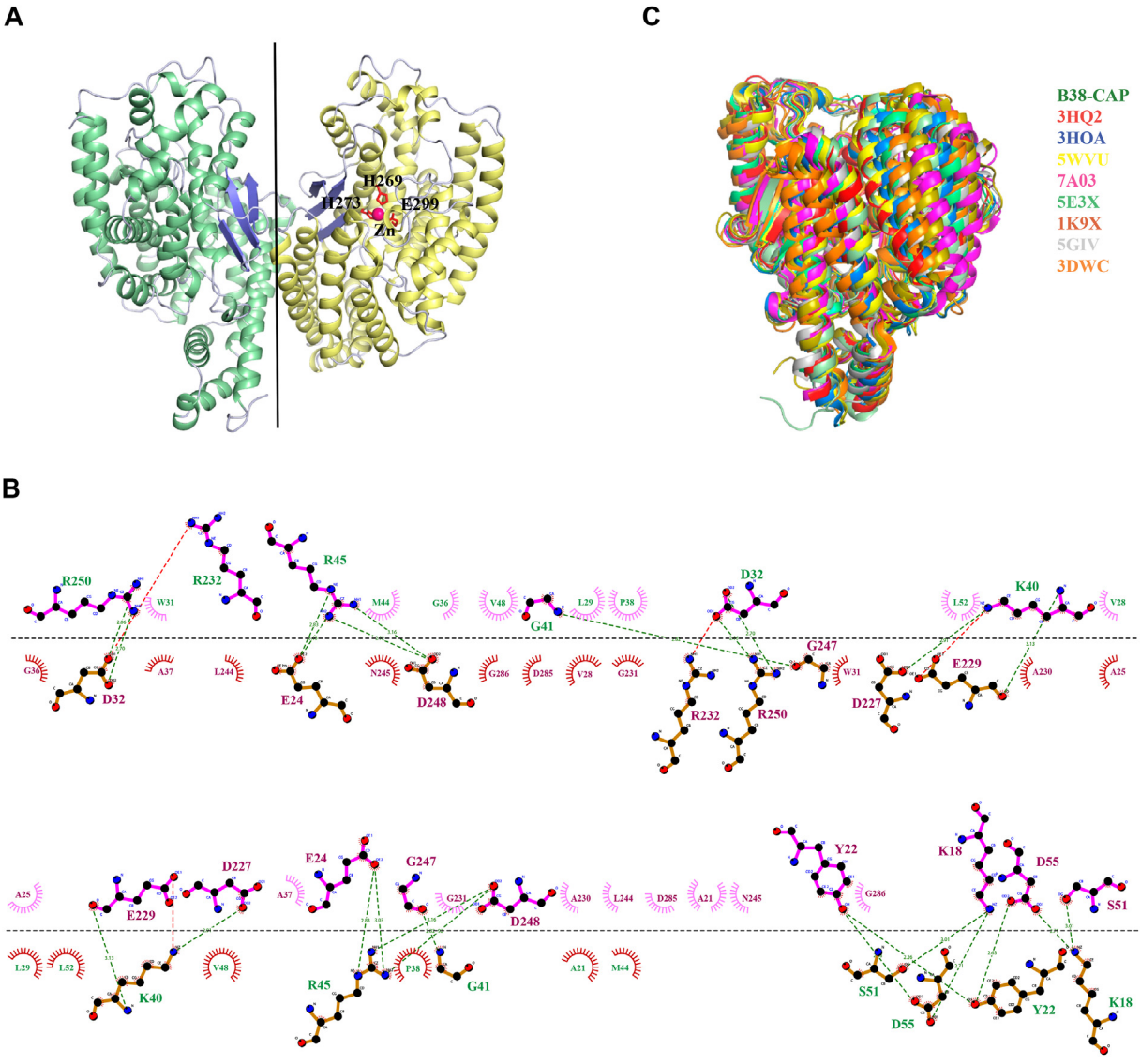

Fig. 2. The overall structure of B38-CAP. **(A)** The dimeric structure of B38-CAP in cartoon representation. **(B)** A close-up view of the interaction on the dimeric interface of B38-CAP. **(C)** Structural alignments between B38-CAP (palegreen) monomer and other carboxypeptidase monomers. PDB entry 3HQ2, 3HOA, 5WVU, 7A03, 5E3X, 1K9X, 5GIV, 3DWC are colored in red, marine, yellow, magenta, lime green, olive, gray and orange, respectively.

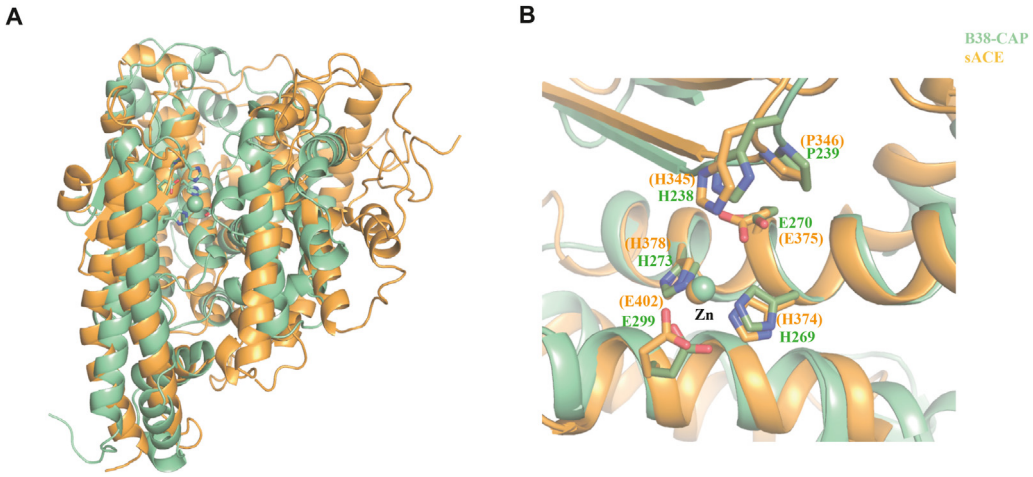

Fig. 3. Structural comparison for (**A**) the overall structure and (**B**) the catalytic core of B38-CAP (palegreen) and ACE2 (bright orange) carboxypeptidase domain.

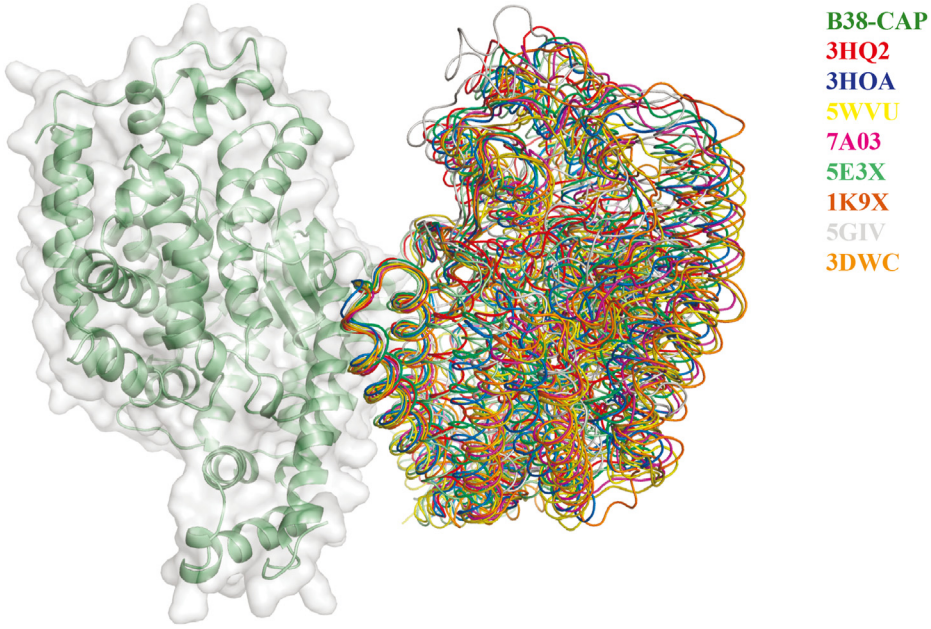

Fig. 4. Structural alignment among B38-CAP and other bacteria-derived carboxypeptidases dimers. Monomer A of all the other bacteria-derived carboxypeptidases were hide after aligned to B38-CAP monomer A, which adopts the same orientation as in Fig. 1A and is shown in cartoon. The monomer B of B38-CAP and all the other bacteria-derived carboxypeptidases were then shown in cartoon, following the color scheme as shown in Fig. 2C.

carboxypeptidase catalysis. The presented high-resolution structure of B38-CAP and corresponding structural comparison with ACE2 help elucidate their structural conservation feature and also their structural diversity and is believed to aid further understanding of the catalytic machinery.

4. Conclusions

In this study, we characterized the dimeric state of B38-CAP which is in accordance with its solved crystal structure. We also characterized the real-time carboxypeptidase activity of B38-CAP which is weaker compared to ACE2. Structural comparison between B38-CAP and other M32-family carboxypeptidase showed highly sequential and structural similarity while only structural conservatism was retained between B38-CAP and ACE2 carboxypeptidase domain, particularly in their catalytic core. Moreover, the dimeric architecture was shown to be strictly conservative among bacteria-derived carboxypeptidases while ACE2 did not obey this rule. This marked difference is considerably worthy of in-depth study and might contribute to a new understanding of the diversity of the catalytic machinery within M32 family carboxypeptidases and also the ongoing development of B38-CAP-based anti-SARS-CoV-2 drugs [30].

Declaration of competing interest

The authors declare that they have no conflicts of interest.

Acknowledgements

We thank all members for technical assistance and helpful discussions. We thank Yong Li in Tianjin University for X-ray facility assistance. This work was supported by grants from National Key Research Program of China (2016YFD0500300); Open Project

Funding of the Key Laboratory of Medical Molecular Virology (MOE/NHC/CAMS) of Fudan University (FDMV-2021001); Open Funding Project of the State Key Laboratory of Biocatalysis and Enzyme Engineering of Hubei University (SKLBEE2021010); the National Natural Science Foundation of China (31600603) and Seed Foundation of Tianjin University (2021XYZ-0003).

Appendix A. Supplementary data

Supplementary data to this article can be found online at https://doi.org/10.1016/j.bbrc.2022.03.077.

References

[1] N. Zhu, D. Zhang, W. Wang, X. Li, B. Yang, J. Song, X. Zhao, B. Huang, W. Shi, R. Lu, P. Niu, F. Zhan, X. Ma, D. Wang, W. Xu, G. Wu, G.F. Gao, W. Tan, A novel coronavirus from patients with pneumonia in China, 2019, N. Engl. J. Med. 382 (2020) 727–733, https://doi.org/10.1056/nejmoa2001017.

[2] A.E. Gorbalenya, M. Krupovic, A. Mushegian, A.M. Kropinski, S.G. Siddell, A. Varsani, M.J. Adams, A.J. Davison, B.E. Dutilh, B. Harrach, R.L. Harrison, S. Junglen, A.M.Q. King, N.J. Knowles, E.J. Lefkowitz, M.L. Nibert, L. Rubino, S. Sabanadzovic, H. Sanfaçon, P. Simmonds, P.J. Walker, F.M. Zerbini, J.H. Kuhn, The new scope of virus taxonomy: partitioning the virosphere into 15 hierarchical ranks, Nat. Microbiol. 5 (2020) 668–674, https://doi.org/10.1038/s41564-020-0709-x.

[3] WHO coronavirus (COVID-19) dashboard. https://covid19.who.int/, 2019. (Accessed 3 March 2022).

[4] P. Ghasemiyeh, S. Mohammadi-Samani, N. Firouzabadi, A. Dehshahri, A. Vazin, A focused review on technologies, mechanisms, safety, and efficacy of available COVID-19 vaccines, Int. Immunopharm. 100 (2021) 1–19, https://doi.org/10.1016/j.intimp.2021.108162.

[5] First oral antiviral for COVID-19, Lagevrio (molnupiravir), approved by MHRA. https://www.gov.uk/government/news/first-oral-antiviral-for-covid-19-lagevrio-molnupiravir-approved-by-mhra, 2021. (Accessed 5 November 2021).

[6] Pfizer's novel COVID-19 oral antiviral treatment candidate reduced risk of hospitalization of death by 89% in interim analysis of phase 2/3 EPIC-HR study. https://www.pfizer.com/news/press-release/press-release-detail/pfizers-novel-covid-19-oral-antiviral-treatment-candidate, 2021. (Accessed 5 November 2021).

[7] C.M. Batista, L. Foti, Anti-SARS-CoV-2 and anti-cytokine storm neutralizing antibody therapies against COVID-19: update, challenges, and perspectives, Int. Immunopharm. 99 (2021) 1–9, https://doi.org/10.1016/j.intimp.2021.108036.

[8] GSK and Vir Biotechnology Announce Sotrovimab (VIR-7831, Receives emergency use authorization from the US FDA for treatment of mild-to-moderate COVID-19 in high-risk adults and pediatric patients, Retrieved, https://investors.vir.bio/news-releases/news-release-details/gsk-and-vir-biotechnology-announce-sotrovimab-vir-7831-receives, 2021. (Accessed 27 May 2021).

[9] Genomic epidemiology of novel coronavirus-Global subsampling. https://nextstrain.org/ncov/gisaid/global?l=clock, 2021. (Accessed 21 September 2021).

[10] A. Khan, T. Khan, S. Ali, S. Aftab, Y. Wang, W. Qiankun, M. Khan, M. Suleman, S. Ali, W. Heng, S.S. Ali, D.Q. Wei, A. Mohammad, SARS-CoV-2 New Variants: Characteristic Features and Impact on the Efficacy of Different Vaccines, Biomedicine and Pharmacotherapy, 143, 2021, pp. 1–11, https://doi.org/10.1016/j.biopha.2021.112176.

[11] S.R. Tipnis, N.M. Hooper, R. Hyde, E. Karran, G. Christie, A.J. Turner, A human homolog of angiotensin-converting enzyme: cloning and functional expression as a captopril-insensitive carboxypeptidase, J. Biol. Chem. 275 (2000) 33238–33243, https://doi.org/10.1074/jbc.M002615200.

[12] M. Hoffmann, H. Kleine-Weber, S. Schroeder, N. Krüger, T. Herrler, S. Erichsen, T.S. Schiergens, G. Herrler, N.H. Wu, A. Nitsche, M.A. Müller, C. Drosten, S. Pöhlmann, SARS-CoV-2 cell entry depends on ACE2 and TMPRSS2 and is blocked by a clinically proven protease inhibitor, Cell 181 (2020) 271–280, https://doi.org/10.1016/j.cell.2020.02.052.

[13] S. Bank, S.K. De, B. Bankura, S. Maiti, M. Das, G.A. Khan, Ace/ace2 balance might be instrumental to explain the certain comorbidities leading to severe covid-19 cases, Biosci. Rep. 41 (2021) 1–6, https://doi.org/10.1042/BSR20202014.

[14] J. Lan, J. Ge, J. Yu, S. Shan, H. Zhou, S. Fan, Q. Zhang, X. Shi, Q. Wang, L. Zhang, X. Wang, Structure of the SARS-CoV-2 spike receptor-binding domain bound to the ACE2 receptor, Nature 581 (2020) 215–220, https://doi.org/10.1038/s41586-020-2180-5.

[15] L. Bitker, L.M. Burrell, Classic and nonclassic renin-angiotensin systems in the critically ill, Crit. Care Clin. 35 (2019) 213–227, https://doi.org/10.1016/j.ccc.2018.11.002.

[16] C. Vickers, P. Hales, V. Kaushik, L. Dick, J. Gavin, J. Tang, K. Godbout, T. Parsons, E. Baronas, F. Hsieh, S. Acton, M. Patane, A. Nichols, P. Tummino, Hydrolysis of biological peptides by human angiotensin-converting enzyme-related carboxypeptidase, J. Biol. Chem. 277 (2002) 14838–14843, https://doi.org/10.1074/jbc.M200581200.

[17] A. Zoufaly, M. Poglitsch, J.H. Aberle, W. Hoepler, T. Seitz, M. Traugott, A. Grieb, E. Pawelka, H. Laferl, C. Wenisch, S. Neuhold, D. Haider, K. Stiasny, A. Bergthaler, E. Puchhammer-Stoeckl, A. Mirazimi, N. Montserrat, H. Zhang, A.S. Slutsky, J.M. Penninger, Human recombinant soluble ACE2 in severe COVID-19, Lancet Respir. Med. 8 (2020) 1154–1158, https://doi.org/10.1016/S2213-2600(20)30418-5.

[18] V. Monteil, H. Kwon, P. Prado, A. Hagelkrüys, R.A. Wimmer, M. Stahl, A. Leopoldi, E. Garreta, C. Hurtado del Pozo, F. Prosper, J.P. Romero, G. Wirnsberger, H. Zhang, A.S. Slutsky, R. Conder, N. Montserrat, A. Mirazimi, J.M. Penninger, Inhibition of SARS-CoV-2 infections in engineered human tissues using clinical-grade soluble human ACE2, Cell 181 (2020) 905–913, https://doi.org/10.1016/j.cell.2020.04.004.

[19] F. Cocozza, E. Piovesana, N. Névo, X. Lahaye, J. Buchrieser, O. Schwartz, N. Manel, M. Tkach, C. Théry, L. Martin-Jaular, Extracellular vesicles containing ACE2 efficiently prevent infection by SARS-CoV-2 Spike protein-containing virus, J. Extracell. Vesicles (2020) 1–8, https://doi.org/10.1101/2020.07.08.193672.

[20] M.L. Yeung, J.L.L. Teng, L. Jia, C. Zhang, C. Huang, J.P. Cai, R. Zhou, K.H. Chan, H. Zhao, L. Zhu, K.L. Siu, S.Y. Fung, S. Yung, T.M. Chan, K.K.W. To, J.F.W. Chan, Z. Cai, S.K.P. Lau, Z. Chen, D.Y. Jin, P.C.Y. Woo, K.Y. Yuen, Soluble ACE2-mediated cell entry of SARS-CoV-2 via interaction with proteins related to the renin-angiotensin system, Cell 184 (2021) 2212–2228, https://doi.org/10.1016/j.cell.2021.02.053.

[21] T. Minato, S. Nirasawa, T. Sato, T. Yamaguchi, M. Hoshizaki, T. Inagaki, K. Nakahara, T. Yoshihashi, R. Ozawa, S. Yokota, M. Natsui, S. Koyota, T. Yoshiya, K. Yoshizawa-Kumagaye, S. Motoyama, T. Gotoh, Y. Nakaoka, J.M. Penninger, H. Watanabe, Y. Imai, S. Takahashi, K. Kuba, B38-CAP is a bacteria-derived ACE2-like enzyme that suppresses hypertension and cardiac dysfunction, Nat. Commun. 1058 (2020) 1–12, https://doi.org/10.1038/s41467-020-14867-z.

[22] M.M. Lee, C.E. Isaza, J.D. White, R.P.Y. Chen, G.F.C. Liang, H.T.F. He, S.I. Chan, M.K. Chan, Insight into the substrate length restriction of M32 carboxypeptidases: characterization of two distinct subfamilies, Proteins: Struct. Function Bioinformat. 77 (2009) 647–657, https://doi.org/10.1002/prot.22478.

[23] P. Emsley, K. Cowtan, Coot: model-building tools for molecular graphics, Acta Crystallogr. Sect. D Biol. Crystallogr. 60 (2004) 2126–2132, https://doi.org/10.1107/S0907444904019158.

[24] P.D. Adams, P.v. Afonine, G. Bunkóczi, V.B. Chen, I.W. Davis, N. Echols, J.J. Headd, L.W. Hung, G.J. Kapral, R.W. Grosse-Kunstleve, A.J. McCoy, N.W. Moriarty, R. Oeffner, R.J. Read, D.C. Richardson, J.S. Richardson, T.C. Terwilliger, P.H. Zwart, PHENIX: a comprehensive Python-based system for macromolecular structure solution, Acta Crystallogr. Sect. D Biol. Crystallogr. 66 (2010) 213–221, https://doi.org/10.1107/S0907444909052925.

[25] C.J. Williams, J.J. Headd, N.W. Moriarty, M.G. Prisant, L.L. Videau, L.N. Deis, V. Verma, D.A. Keedy, B.J. Hintze, V.B. Chen, S. Jain, S.M. Lewis, W.B. Arendall, J. Snoeyink, P.D. Adams, S.C. Lovell, J.S. Richardson, D.C. Richardson, MolProbity: more and better reference data for improved all-atom structure validation, Protein Sci. 27 (2018) 293–315, https://doi.org/10.1002/pro.3330.

[26] L. Holm, L.M. Laakso, Dali server update, Nucleic Acids Res. 44 (2016) W351–W355, https://doi.org/10.1093/nar/gkw357.

[27] W.L. Delano, The PyMOL molecular graphics system, Proteins Struc. Function Bioinformat. 30 (2002) 442–454. http://www.pymol.org.

[28] S. Takahashi, T. Yoshiya, K. Yoshizawa-Kumagaye, T. Sugiyama, Nicotianamine is a novel angiotensin-converting enzyme 2 inhibitor in soy-bean, Biomed. Res. 36 (2015) 219–224, https://doi.org/10.2220/biomedres.36.219.

[29] P. Towler, B. Staker, S.G. Prasad, S. Menon, J. Tang, T. Parsons, D. Ryan, M. Fisher, D. Williams, N.A. Dales, M.A. Patane, M.W. Pantoliano, ACE2 X-ray structures reveal a large hinge-bending motion important for inhibitor binding and catalysis, J. Biol. Chem. 279 (2004), https://doi.org/10.1074/jbc.M311191200, 17996–18007.

[30] T. Yamaguchi, M. Hoshizaki, T. Minato, S. Nirasawa, M.N. Asaka, M. Niiyama, M. Imai, A. Uda, J.F.W. Chan, S. Takahashi, J. An, A. Saku, R. Nukiwa, D. Utsumi, M. Kiso, A. Yasuhara, V.K.M. Poon, C.C.S. Chan, Y. Fujino, S. Motoyama, S. Nagata, J.M. Penninger, H. Kamada, K.Y. Yuen, W. Kamitani, K. Maeda, Y. Kawaoka, Y. Yasutomi, Y. Imai, K. Kuba, ACE2-like carboxypeptidase B38-CAP protects from SARS-CoV-2-induced lung injury, Nat. Commun. 12 (2021) 1–13, https://doi.org/10.1038/s41467-021-27097-8.